Prediction of Neuroprotective Treatment Efficiency Using a HRMAS NMR-Based Statistical Model of Refractory Status Epilepticus on Mouse: A Metabolomic Approach Supported by Histology

Florence Fauvelle, Pierre Carpentier, Frederic Dorandeu, Annie Foquin, Guy Testylier

Journal of proteome research

Article

pubs.acs.org/jpr

Prediction of Neuroprotective Treatment Efficiency Using a HRMAS NMR-Based Statistical Model of Refractory Status Epilepticus on Mouse: A Metabolomic Approach Supported by Histology

Florence Fauvelle,*[,†] Pierre Carpentier,[‡] Frederic Dorandeu,[‡,§] Annie Foquin,[‡] and Guy Testylier[‡]

[†]Département Effets Biologiques des Rayonnements, IRBA-CRSSA, La Tronche, France

[‡]Département de Toxicologie et Risques Chimiques, IRBA-CRSSA, La Tronche, France

[§]Ecole du Val-de-Grâce, Paris, France

ABSTRACT: This work presents a model combining quantitative proton HRMAS NMR data and PLS-DA for neuropathology and neuroprotection evaluation. Metabolic data were also confronted to histopathological results obtained using the same experimental conditions. Soman, when not lethal, can induce status epilepticus (SE), brain damage, histological lesions, and profound cerebral metabolic disorders as revealed using ^{1}H HRMAS NMR. Our challenge was to evaluate delayed treatments, which could control refractory SE and avoid brain lesions. For this aim, we have built a statistical model of soman intoxication describing brain metabolite evolution during 7 days. We have then used this model to evaluate the efficiency of a combination of ketamine/atropine (KET/AS) administrated 1 and 2 h after SE induction, compared to the immediate anticonvulsant therapy midazolam/atropine sulfate (MDZ/AS). Furthermore, quantitation of HRMAS NMR data allowed us to follow individual evolution of 17 metabolites. *N*-Acetylaspartate, lactate, or taurine presented a long lasting disruption, while glutamine, alanine, glycerophosphocholine and myo-inositol showed disruptions for 3 days with a reversion at day 7. These changes were completely normalized by the administration of MDZ/AS. Interestingly, they were also almost completely reversed by KET/AS 1 h postsoman. This work suggests further the predictive interest of HRMAS and PLS-DA for neuropathology/neuroprotection studies and also confirms, on the metabolic aspects, the neuroprotective potentials of KET/AS combinations for the delayed treatment of soman-induced SE.

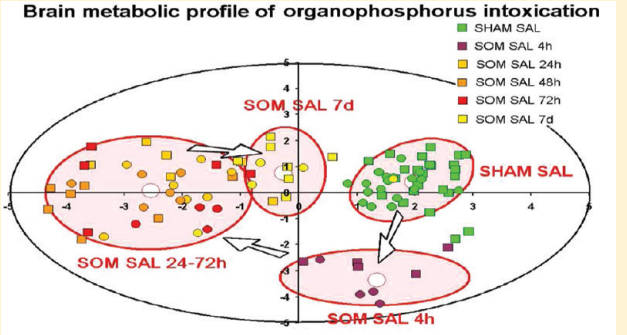

KEYWORDS: *soman, ketamine, midazolam, high resolution magic angle spinning, PLS-DA, brain histology*

INTRODUCTION

Soman is an organophosphorus nerve agent that acts as an irreversible inhibitor of acetylcholinesterase both in central and in peripheral nervous systems. This leads to a massive hypercholinergy resulting in hypersecretion, respiratory distress, convulsive seizures and rapid death if the dose is sufficient.[1] Although soman-induced seizures primarily stem from cholinergic overstimulation,[2] their maintenance is mainly attributable to a secondary massive release of glutamate,[1] an excitatory amino acid that has been recognized for its "excitotoxic" potential.[3] In survivors, seizure activity may evolve into a *status epilepticus* (SE) that becomes refractory to benzodiazepines if not quickly stopped. Numerous sensitive brain areas such as cortex, piriform cortex, amygdala, septum, thalamus or hippocampus may end up showing seizure-related brain damage (SRBD).[4−7] Survivors of these severe intoxications may suffer from neurological sequelae such as spontaneous recurrent seizures[8] after a latent period of epileptogenesis, as well as cognitive deficits.[9,10] Numerous pathological events are known to accompany SRBD. For instance, a cytotoxic and vasogenic cerebral edema develops within a few hours after poisoning[11,12] and neuroinflammation occurs in the hours or days following SE as evidenced through the appearance of astro- and microgliosis,[4,13] recruitment of peripheral immune cells[14,15] and synthesis of various molecular markers such as cytokines and cell adhesion molecules.[16−18]

Moreover, SE, would it be soman-induced or of a different origin,[19−21] can trigger major disturbances of brain metabolism including changes in the energy,[22,23] aminoacid[24] and phospholipid metabolisms.[25,26] To explore further cerebral metabolic changes after soman, we recently used proton high resolution magic angle spinning (^{1}H HRMAS) nuclear magnetic resonance (NMR) spectroscopy (HRMAS NMR).[27] This technique, which has been successfully applied in various tissues and diseases,[28−31] allows the characterization of the metabolic phenotypes of cells, tissues and organs under both normal and pathological conditions, without any extraction or chemical treatments. Therefore, it offers the advantage of eliminating the contamination associated with extraction

Received: March 26, 2012

dx.doi.org/10.1021/pr300291d | *J. Proteome Res.* XXXX, XXX, XXX−XXX

procedures. With this method applied ex vivo to brain biopsies from mice, we were able in our previous work to quantitate using the jMRUI software (www.jmrui.uab.es/mrui/) 17 metabolites up to 7 days after soman-induced SE.[27] While only 2 metabolites were modified in the cerebellum, a structure that apparently remains structurally intact in soman-intoxicated mice, 13 showed significant changes in the piriform cortex. In the latter, changes could be detected as soon as 4 h postchallenge, but with the notable exception of *N*-acetylaspartate (NAA), lactate and taurine, metabolite levels were normalized after one week. Some of the observed metabolic disorders could be tentatively related to postsoman, SE-related pathophysiological events.[27] For instance, NAA decrease may be considered as a marker of neuronal loss or neuronal mitochondrial dysfunctions.[32] The large increase of lactate observed from 24 to 72 h after intoxication could also be associated with mitochondrial dysfunction.[33] Myo-inositol and taurine are among the main osmolytes in the brain, and their decrease could be related to the observed brain edema.[34,35] Glycerophosphocholine increase could be associated to phospholipase activation during neuroinflammatory process induced by seizures.[36]

In this previous work,[27] HRMAS NMR quantitative data were also submitted to multivariate statistical analysis. These methods, such as principal component analysis (PCA) and projection to latent structure-discriminant analysis (PLS-DA), allow one to reduce the number of variables (i.e., 17 NMR variables in our case) to two or three supervariables (latent variables) that define a new space in which observations are projected. This provides an important help to describe data and to find "metabolic profiles" characteristic of a given status or pathology. Moreover, if the model is sufficiently robust, it could allow predicting the classification of an unknown observation from its NMR spectrum. We clearly showed metabolic differences between damaged and less damaged brain structures and helped to globally assess the time course of metabolic changes. This study, bridging soman-induced SRBD and metabolic disorders, suggested that quantitation of HRMAS NMR data associated with PLS-DA analysis might be useful to provide temporal and local metabolic signatures of soman poisoning, and possibly markers for neuropathology and clues to explain pathophysiological mechanisms.

The standard treatment against organophosphorus intoxication combines an antimuscarinic drug such as atropine sulfate (AS) and an oxime that reactivates the inhibited cholinesterase (e.g., HI6). Benzodiazepines like diazepam or midazolam (MDZ) are used to stop seizures. The combination of HI6, AS and MDZ (MDZ/AS) constitute the "antidote" used by the French army, but this combination needs to be very quickly administered, preferably within ca. 20 min after seizure onset, to provide the best protection against SRBD and long-term neurological deficits.[37−41] Indeed, if the continuous seizures are left unabated, they will not respond well to benzodiazepines, and the SE becomes refractory. The management of refractory SE (RSE) is a therapeutical challenge and constitutes one of the main goals of our research.

Drug combinations of ionotropic glutamate receptor antagonists (NMDA antagonists or AMPA antagonists) are among the most efficient drugs. In experimental soman poisoning and SE, NMDA antagonists such as MK-801,[42,43] TCP,[44,45] GK-11[46] showed promising effects, most of the time when associated with AS. Unfortunately, these drugs are either not usable in humans because of severe adverse effects or have not been licensed. Ketamine (KET) is the only NMDA antagonist licensed as an injectable drug in different countries. It is commonly used in emergency care and military anesthesiology. It has little effect on the cardiovascular system and does not easily induce respiratory depression. It is recognized as a possible third line treatment of RSE.[47,48] It also exerts peripheral anti-inflammatory properties.[49,50] In guinea pigs, KET in combination with AS was shown to stop seizures and drastically reduce brain damage even when administered ca. 1 h after seizure onset,[51] a property shared by the active isomer S(+) KET.[52] With a comparable paradigm, KET/AS combinations were also shown to reduce brain damage and neuroinflammation in poisoned mice.[15] However, KET/AS administered 2 h after soman provided very limited neuroprotective effects.[51]

These data show that KET combinations could constitute an efficient delayed treatment of soman intoxication when SE becomes refractory to benzodiazepine treatment. In this study we have used a metabolomic approach to evaluate the effect of KET treatments on brain damage. For this aim, we first built a robust multivariate statistical "soman model". Statistical power was increased by combining new metabolic data with data of our previous study.[27] Second, three treatments were tested: the classical "antidote" administered immediately after soman (MDZ/AS) and two delayed treatments with KET/AS at 1 and 2 h. The MDZ/AS treatment constituted a positive control to evaluate the predictability of our statistical "soman model", which was then used to evaluate efficiency of delayed KET treatments. In parallel to the HRMAS NMR analysis, a classical histological study was performed.

Furthermore, the quantitation of HRMAS NMR data allowed us to associate metabolic disorders to the various events occurring during and after the intoxication, and to identify more precisely the mechanism of action of treatments.

Finally, this study could contribute to support the use of HRMAS NMR-based metabolomics as a predictive tool for neuropathology and neuroprotection in preclinical studies.

MATERIALS AND METHODS

Animals

Male Swiss mice (32.9 ± 2.0 g; Elevage Janvier, France) were used in the present study. They were housed in a controlled environment (21 ± 2 °C; 12 h dark/light cycle with light provided between 7 a.m. and 7 p.m.). Food and water were given ad libitum. All procedures followed were in accordance with the regulations regarding the "protection of animals used for experimental and other scientific purposes" from the relevant Directive of the European Community (86/609/CEE) and French legislation. The present protocol was approved by the Ethical Committee of our Institute.

Drugs

Soman (>97% pure as assessed by gas chromatography) was supplied by the Centre DGA maîtrise NRBC du Bouchet (Vert-le-Petit, France). Solutions were freshly prepared by diluting the initial stock solution (2 mg/mL in isopropanol) in 0.9% (w/v) saline prior to the injection. The oxime HI6 dichloride was a generous gift of DRDC Suffield (Canada). Methylatropine nitrate and atropine sulfate (AS) were purchased from Sigma Chemicals (France). Midazolam (MDZ) and ketamine (KET) were purchased from Panpharma SA (France).

dx.doi.org/10.1021/pr300291d | J. Proteome Res. XXXX, XXX, XXX−XXX

Experimental Design

Mice were pretreated with HI6 dichloride (50 mg/kg i.p.) and methylatropine nitrate (4 mg/kg i.p.), 5 min prior to either soman (172 μg/kg ca. 0.6 LD_{50} in the presence of HI-6 pretreatment, s.c. in the nape of the neck) or saline injection (200 μL, s.c.). The oxime HI6 dichloride, an acetylcholinesterase reactivator, and methylatropine nitrate, an antagonist of peripheral muscarinic receptors, were used to limit lethality due to respiratory distress.

This protocol is identical or very similar to those routinely used in our laboratory[4,11,15,16,27] and can serve as a model for RSE with a high survival rate in absence of any therapy. For the two challenge conditions, either intoxication with soman (SOM groups) or no intoxication (SHAM groups), four different treatment protocols were considered, leading to eight groups:

(1) Classical "antidote" treatment (MDZ/AS): SOM MDZ/AS and SHAM MDZ/AS groups. This protocol efficiently controls seizures when administered immediately after challenge. MDZ (25 mg/kg) and AS (10 mg/kg) were administered i.p. only once in two separate injections.

(2) Ketamine 1 h treatment (KET1h/AS): SOM KET1h/AS and SHAM KET1h/AS groups. This protocol controls the RSE when administered for the first time 1 h after challenge. KET (100 mg/kg) and AS (10 mg/kg) were administered in two separate injections 1 h after intoxication. At 2 and 3 h postchallenge, KET (50 mg/kg) and AS (10 mg/kg) were injected i.p. in two separate injections.

(3) Ketamine 2 h treatment (KET2h/AS): SOM KET2h/AS and SHAM KET2h/AS groups. This protocol does not properly control the refractory SE when administered 2 h after challenge. The same protocol as KET1h was used but started 2 h after challenge.

(4) Control protocol: SOM SAL and SHAM SAL groups. Three injections of saline (200 μL i.p.) replaced the treatments, one injection every hour starting 1 h after challenge (to match the KET/AS groups where the treatments were administered three times).

All animals were observed for 6 h postchallenge, and the signs and symptoms of the intoxication were recorded. Mice were weighed just before any treatment and every day postchallenge until euthanized. The body weight loss after soman poisoning may be considered as a good indicator of the global health status of the mice and a surrogate marker of central damage.[9,15,52,53]

Histological Analysis

For this study, no SHAM groups were considered. Four groups (n = 21 each) were intoxicated with soman and received one of the treatments previously described (SOM SAL, SOM MDZ/AS, SOM KET1h/AS, SOM KET2h/AS). For each group, the animals were euthanized either 24 h (n = 7), 72 h (n = 7) or 7 days (n = 7) after intoxication. Mice were deeply anesthetized (sodium pentobarbital, 80 mg/kg; i.p.) and transcardially perfusion-fixed with a mixture of formaldehyde (4%) and acetic acid (3%). Coronal blocks of brain, from +2 to −2.5 mm (containing the piriform cortex and the amygdala), and from −5.5 to −7 mm (containing a part of the cerebellum) relative to bregma, were embedded in paraffin. Histological sections (7 μm thick) chosen for analysis were situated approximately either −1.94 or −6 mm relative to bregma.[54] They were stained with Hemalun−Phloxin (HP) for the detection of damaged (eosinophilic) cells, appearing in dark violet. On adjacent sections, reactive astrocytes were revealed by glial fibrillary acidic protein (GFAP) immunohistochemistry using a protocol previously described.[15]

Equally magnified (20×), high resolution (1.25 Mpixels, 48 bit colors), digital images (690 × 520 μm) from the amygdaloid nucleus, the piriform cortex and the dorsal cerebellar lobule from each mouse were acquired with an Axio Imager Z1 Zeiss microscope equipped with an Axiocam MR5 camera (Zeiss, Germany). Eosinophilic cells and astrocytes were identified on the basis of their color, shape and size and quantitated using the Axiovision image processing software (vs 4.6.3.0). Quantitation was achieved as previously described:[15] within each chosen brain structure, the number of eosinophilic cells on the HP-stained sections and the percentage of the surface occupied by GFAP positive cells on the GFAP-treated sections were determined. The results are expressed as the mean ± SEM calculated for each group and at each time point.

^{1}H HRMAS NMR Spectroscopy

Biopsy Preparation. For each group and each time point, 5−9 mice depending on the group size were euthanized 4, 24, 48, or 72 h and 7 days after challenge. Mice were decapitated, and their brains were rapidly removed and dissected on ice for the preparation of HRMAS biopsies. Two samples were chosen: the first contained the piriform cortex and amygdala (PIR/AMG) from both hemispheres, as severely damaged areas; the second was the cerebellum (CER), an area that remains apparently structurally intact. These biopsies were obtained using a coronal dissection matrix allowing the dissection of slices (2−3 mm thick) located from +0.5 to −2.5 mm (for PIR/AMG) or from −5.5 to −7.5 mm (for CER) relative to the bregma. They were immediately frozen in liquid nitrogen. Approximately 15 mg of the frozen biopsies were used for each assay.

HRMAS Data Acquisition. Proton NMR spectra were recorded on a Bruker Avance 400 spectrometer (proton frequency 400.13 MHz) equipped with a 4 mm ^{1}H−^{13}C−^{31}P HRMAS probe-head. Samples were spun at 4000 Hz. 1D spectra were all acquired with a Carr−Purcell−Meiboom−Gill (CPMG) pulse sequence to attenuate macromolecule and lipid resonances, synchronized with the spinning rate (interpulse delay 250 μs, total spin echo time 30 ms). Residual water signal was presaturated during the 2 s relaxation delay time. Total acquisition of one spectrum with 256 scans lasted 16 min. Resonance assignment was performed as previously described.[55]

Data Processing. Quantitation was performed with the package software jMRUI using the "subtract-QUEST" procedure.[56] This procedure uses a simulated metabolite database (for details, see Rabeson[55]). Twenty-one metabolites were included in the database: acetate (Ace), alanine (Ala), aspartate (Asp), creatine and phosphocreatine (Cr), choline (Cho), ethanolamine (Eth), γ-amino-butyric acid (GABA), glutamate (Glu), glutamine (Gln), glutathione (Gsh), glycerophosphocholine (GPC), glycine (Gly), lactate (Lac), myo-inositol (M-ins), N-acetylaspartate (NAA), phosphoethanolamine (PE), phosphocholine (PC), scyllo-inositol (S-ins), serine (Ser), taurine (Tau) and valine (Val). The amplitude of each metabolite signal calculated by QUEST was normalized to the total spectrum signal. The Cramer Rao lower bounds (CRLB) calculated by the jMRUI algorithm are estimates of the

dx.doi.org/10.1021/pr300291d | J. Proteome Res. XXXX, XXX, XXX−XXX

standard deviation of the fit for each metabolite. For 17 metabolites, CRLB was either ≤5 or ≤25% (Ace, Asp). They were all included in the statistical analysis. Only four metabolites (Eth, S-ins, Ser and Val), showed a CRLB ≥ 50% and were excluded from the statistical analysis.

Statistical Analysis

Univariate Statistical Analysis. All metabolic data, image quantitations or body weight changes are expressed as mean ± SEM. Data were analyzed using the Kruskall Wallis ANOVA by ranks to compare the different post treatment groups. These tests were followed by a post hoc multiple comparison test: at each time, treated groups (MDZ/AS, KET1h/AS, KET2h/AS) were compared to the SHAM groups or to the intoxicated, untreated mice (SOM SAL group) (Statistica v. 6.1 software, Statsoft, Inc.). The level of significance was set at $\alpha = 5\%$.

Multivariate Statistical Analysis. *Statistical Model of Soman Intoxication ("Soman Model").* The statistical model of soman intoxication, named "soman model", was built with data from the SOM SAL and SHAM SAL groups and from our previous study.[27] The only difference between the two studies consists in the injection of saline in the present work, which was not used in the previous one. The amplitude of each metabolite quantitated after HRMAS analysis were then imported into the SIMCAP V12 software (Umetrics AB, Umea, Sweden) as X variables. They were mean centered, scaled to unit variance (i.e., weighted by 1/standard deviation for a given variable) and grouped in a first principal component analysis (PCA), resulting in a total matrix of 102 observations (mice) and 17 variables. This allows us to rapidly evaluate quality and homogeneity of data and to find clusters for further supervised statistical analysis. It appeared that the observations of the previous[27] and present HRMAS studies were well grouped, even if some differences could be observed for some variables individually (see the Results section). Consequently, all data were included in the model to increase its statistical power.

Then partial least square discriminant analyses (PLS-DA)[57] were run with the clusters that appeared in PCA analysis as Y variables, in order to build a model that optimizes the separation between them. The number of components was determined using the cross validation procedure that produces R^2Y and Q^2 factors. The R^2Y value indicates the goodness of fit, while the Q^2 value is a measure of the predictability of the model. It is generally considered that $R^2Y > 0.5$ and $Q^2 > 0.5$ are decent values.

In order to obtain an estimate of the significance of the Q^2 value, the model was validated using random permutations of the Y matrix (999 permutations). For each permuted Y, Q^2 is recalculated, and the correlation coefficients between the original Y and the permuted Y versus the cumulative Q^2 are represented by a regression line whose value to the origin must be negative, indicating the absence of any overfitting in the model.[58] The same procedure is applied to R^2Y values.

Moreover, the reliability of our PLS-DA model was assessed by a CV-ANOVA test (analysis of variance testing of cross-validated predictive residuals). With this method, the metabolites also received a variable importance in the projection (VIP) that allows ranking them according to their contribution to the model.

Prediction of Treatment Efficacy Using the "Soman Model". Finally, we compared the output of the model with the actual results obtained following the administration of the neuroprotective treatments. Treated animals, intoxicated or not, were imported in the model with no a priori class assignment, and the score scatter plots drawn for graphical inspection. These observations were classified using the vicinity criterion. Moreover, the classification rate (in percentage) in the SHAM SAL group was produced to evaluate the efficacy of the treatment.

RESULTS

Clinical Course of the Animals

Mice from SHAM SAL group did not present any behavioral modification after any of the injections. Mice from the SHAM MDZ/AS group presented a sedation lasting 3−4 h after treatment, and mice from KET/AS groups presented sedation between the first and the second injection and during 30−45 min after the second and the third injection. The first KET injection was performed with a high anesthetic dose (100 mg/kg). Despite the use of a reduced dosage for the second and third administration, 8% of the mice treated with the KET/AS protocol alone died, presumably from a KET overdose or because of the combination with AS.

Whatever their treatment, SHAM mice only showed a very limited loss of their body weight at 24 h followed by complete recovery of the prechallenge weight at 48 h. Weight then regularly increased during the following days.

The immediate administration of an anticonvulsant therapy (MDZ/AS) to soman poisoned mice prevented the appearance of convulsions and induced a quick sedation. Only small fasciculation could be observed in 60% of the mice. Their body weight loss was limited (ca. 10% at 24 h), and a complete recovery of body weight was observed at day 7.

Conversely, without the MDZ/AS treatment (animals from the groups SOM SAL, SOM KET1h/AS and SOM KET2h/AS), strong continuous convulsions appeared 3−8 min after soman intoxication in 80% of the mice, while 20% presented discontinuous convulsions. When no treatment was given (SOM SAL group) convulsions lasted for 4−8 h with a decreasing intensity. Twenty-five percent of these animals died between 10 min to 6 h after intoxication. The survivors experienced a drastic body weight loss (Figure 1), reaching about −20% two days postchallenge and very poor recovery in the following days (−12% at day 7). All mice from the SOM KET1h/AS and SOM KET2h/AS groups convulsed until the first injection of KET; convulsions then disappeared when sedation started. In some mice of the SOM KET2h/AS group, convulsions reappeared when the sedation waned between two subsequent KET injections. 7 and 9% of the mice from SOM KET1h/AS and SOM KET2h/AS groups died from intoxication before the first injection of KET/AS, and 7 and 14% died after KET/AS treatment. Interestingly, the body weight loss of surviving animal treated 1 h after soman (SOM KET1h/AS) was similar to that of the MDZ/AS group (ca: −10% at 24 h) but with only a partial recovery (−4% at day 7). Conversely, the body weight loss of animal treated 2 h after soman (SOM KET2h/AS) was comparable to that of mice not receiving any treatment (SOM SAL) at 24 h (−17%) but with a better recovery (−7% at day 7).

Brain Histology

In the SOM SAL group, HP-stained sections of PIR and AMG showed numerous eosinophilic cells 24 h (92 ± 12 and 200 ± 12 stained cells per micrograph, respectively) and 72 h postchallenge (83 ± 17 and 194 ± 29 stained cells per micrograph, respectively) (Figure 2A,B). At day 7, the number

dx.doi.org/10.1021/pr300291d | J. Proteome Res. XXXX, XXX, XXX−XXX

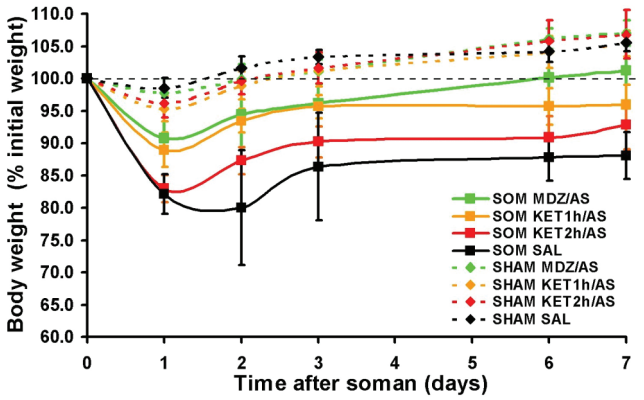

Figure 1. Evolution of the body weight of mice, either challenged with soman (SOM) or saline (SHAM), and then receiving one of the four treatments: saline (SAL), MDZ/AS, KET1h/AS, or KET2h/AS. Mice used for the HRMAS experiments are presented. For each group and at each time, results are expressed as the mean ± SEM of the percentage of the initial body weight (n = 28 in each group at the beginning of the experiment; 7 mice were then taken out at each analysis time). At each time, all points of SOM groups were significantly different from the SHAM SAL group ($p < 0.001$) except at 6 and 7 days for the SOM MDZ/AS group.

of these damaged cells either continued to increase (PIR: 161 ± 51 stained cells) or tended to decrease (AMG: 94 ± 26 stained cells). An astrocytic activation, already important at 72 h, and even stronger at day 7, was detected in AMG. In PIR, the astrocytic activation was comparatively delayed, appearing only at day 7. In the CER neither damaged cells nor astrocytic activation were observed (Figure 2A,B).

When seizures were prevented or immediately stopped (MDZ/AS group), PIR and AMG were devoid of any HP-detectable brain damage or of any astrocytic activation (Figure 2A,B).

Compared to the SOM SAL group, the number of eosinophilic cells in the PIR and AMG from the KET1h/AS and KET2h/AS groups, although showing grossly similar temporal profiles, was either considerably reduced (KET1h/AS: 70−80% decrease of the number of stained cells) or moderately reduced (KET2h/AS: 30−45% decrease of the number of stained cells) for any of the time points. GFAP immunoreactivity in sections of the KET1h/AS and KET2h/AS groups, 72 h postchallenge (important in the AMG; almost negligible in the PIR), were similar to that seen in the SOM SAL group at the same time point and location. However, compared to the important GFAP immunoreactivity seen at day 7 in the SOM SAL group, KET/AS treatment had a clear impact and reduced the GFAP immunoreactivity area: −70 to −80 and −40% in the KET1h/AS and KET2h/AS groups respectively.

In all groups, CER was devoid of any apparent damaged cells and of astrocytic activation.

Temporal Profile of the Metabolite Changes

Effect of the Treatment Paradigms in Nonpoisoned Mice. Compared to mice of the SHAM SAL group, none of the anticonvulsant treatments appeared to induce any long-lasting changes in brain metabolite levels in PIR/AMG or CER. In Figure 3 and 4, only the SHAM SAL group is thus presented. However, at 4 h, during sedation, there was a significant decrease of Glu in PIR/AMG in the three treatment groups (SHAM MDZ/AS: −14%, SHAM KET1h/AS: −14% and SHAM KET2h/AS: −18%).

Effect of Soman and Soman-Induced Seizures (SOM SAL vs SHAM SAL). In the PIR/AMG, 13 metabolites significantly varied in the SOM SAL group as compared to the SHAM SAL group, in accordance with our previous work.[27] We focused in this paper on 8 of them that could be more easily related to pathophysiological events, since they showed the most important changes and received the highest VIP values (see next paragraph, multivariate statistical analysis): Lac, lactate; Gln, glutamine; Ala, alanine; Ace, acetate; GPC, glycerophosphocholine; NAA, *N*-acetylaspartate; M-ins, myo-inositol; and Tau, taurine. The other metabolites were presented and discussed in our previous paper.[27]

A long-lasting increase of Lac was noted from 24 h to day 7 postsoman, with a maximal increase (+55%) after 72 h. Although decreasing thereafter, Lac level remained well above that measured in the SHAM SAL group (Figure 3A). Gln (Figure 3B) significantly increased at 24 h and reached a maximal elevation at 48 h (+36%). It then decreased to reach an almost normal value at day 7. An increase of Ala (Figure 3C) was noted as soon as 4 h post soman, peaking at 48 h (+107%), and decreasing thereafter to the control level at day 7. A significant but transient increase (+95%) of Ace occurred, appearing only 4 h postchallenge (Figure 3D). An increase of GPC (Figure 3E) was also detected, reaching a plateau at 24 h (about +40%) until 72 h, before complete normalization at day 7. NAA levels (Figure 3F) apparently decreased over time with the lowest level being recorded at 72 h (−43%) and were significantly different from the nonpoisoned animals. Despite a tendency to reincrease afterward, NAA level was still far from a complete normalization at day 7 (−27%). As for NAA, M-ins (Figure 3G) also decreased, and the lowest level was observed from 24 to 72 h (about −30 to 35%) before complete normalization at day 7. Finally, Tau (Figure 3H) slightly, but continuously, tended to decrease over the duration of the experiment, with the drop reaching statistical significance only at day 7 (−14%).

The CER of poisoned mice showed only limited changes compared to the SHAM SAL group: a significant decreases of NAA (−15%) at 72 h (Figure 4C) and of M-ins (−13%) at 24 h (Figure 4D).

Effect of the Nature and Timing of Administration of the Anticonvulsant Treatments (SOM MDZ/AS, SOM KET1h/AS, SOM KET2h/AS vs SOM SAL and SHAM SAL). *Effects of an Immediate Seizure Arrest (SOM MDZ/AS Group).* In the PIR/AMG, the immediate therapy prevented or reversed all the metabolic disturbances observed in poisoned animals. In the CER, the very limited soman-induced changes were also abated.

Effects of a 1 h Delay in KET/AS Treatment Initiation. KET/AS treatment, given 1 h after soman poisoning, could also normalize soman-induced changes of 5 out of the 8 metabolites of interest (Lac, Gln, Ace, M-ins and Tau) in PIR/AMG. Conversely, the protection afforded by KET1h/AS appeared incomplete for the other three metabolites, viz. Ala, GPC and NAA. For Ala (Figure 4B), a complete normalization was obtained at 4 and 24 h. However, at 48 h (+43%) and 72 h (+48%), although lower than in the SOM SAL group, the level remained above the control values observed in the SHAM SAL group, with the difference being significant only at 72 h. For GPC (Figure 3E), although the significant increase at 24 h postchallenge remained, the delayed treatment appeared to

dx.doi.org/10.1021/pr300291d | J. Proteome Res. XXXX, XXX, XXX−XXX

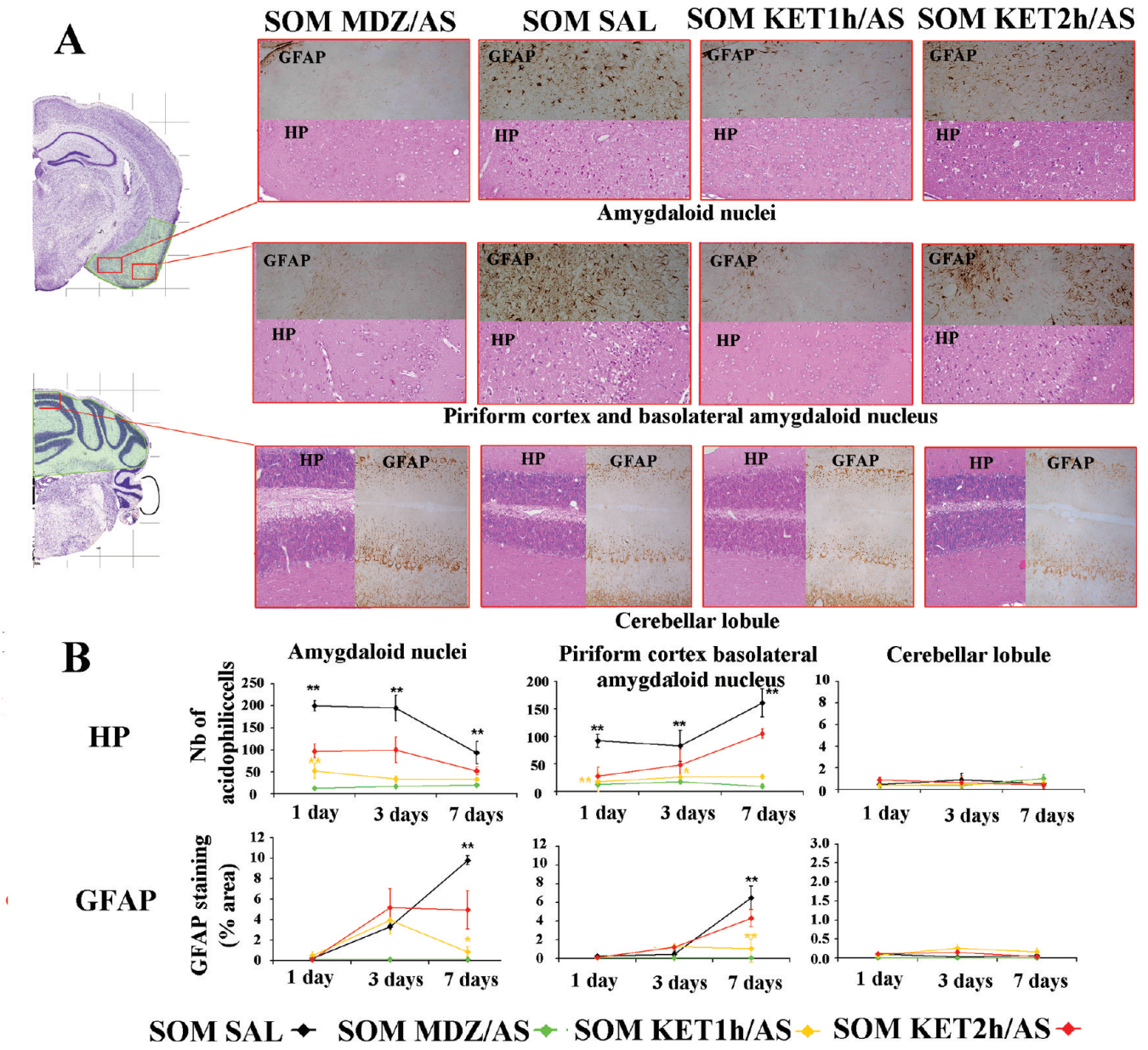

Figure 2. (A) Plates of coronal sections taken from Paxinos and Franklin mouse brain atlas.[54] The red rectangles are the areas chosen to acquire the micrographs. Examples of micrographs 3 days (HP) or 7 days (GFAP) postchallenge from SOM SAL, SOM MDZ/AS, SOM KET1h/AS, and SOM KET2h/AS groups. The green zones on the coronal diagrams are the locations of the biopsies used in the HRMAS study. (B) Quantitative histology. On the HP-stained sections, the number of eosinophilic cells per microphotograph was counted and expressed as the mean ± SEM (n = 7 for each time and each group). On the sections processed for GFAP immunohistochemistry, the percentage of the microphotograph area occupied by reactive astrocytes was measured and expressed as the mean value ± SEM (n = 7 for each time and each group). The diagrams show the results obtained in the amygdala, piriform cortex, and cerebellum of the SOM SAL (black curves), MDZ/AS (green curves), KET1h/AS (orange curves), and KET2h/AS (red curves) groups. Groups were statistically compared by an ANOVA per ranks followed by a posthoc test: black ** $p < 0.01$ between SOM SAL and SOM MDZ/AS groups, and orange ** $p < 0.01$, *$p < 0.05$ between SOM KET1h/AS and SOM SAL groups.

progressively normalize GPC levels (+22 and +16% at 48 and 72 h in the SOM KET1h/AS group vs +39 and +38% at the same time points in the SOM SAL group). For NAA, a decrease was recorded in the SOM KET1h/AS group with, compared to the SOM SAL group, similar temporal profile but with reduced values (maximal change: −13% at 72 h in the SOM KET1h/AS group vs −43% in the SOM SAL group). In the CER, the very limited soman-induced changes were no more detectable.

Effects of a 2 h Delay in KET/AS Treatment Initiation. In PIR/AMG, when the initiation of treatment was further delayed, only one metabolite, Ace, showed a return to control levels (Figure 3A). For GPC, no difference appeared with KET1h/AS group. For the six other metabolites (Lac, M-ins, NAA, Gln, Ala, Tau), they grossly followed the same temporal profiles as those observed in the group of nontreated animals (Figure 3). However, although the amplitude of variation (decrease or increase depending on the metabolite) was reduced, the metabolite levels never significantly differed from those of the SOM SAL group and often remained significantly different from those of the SHAM SAL group. As for the other

dx.doi.org/10.1021/pr300291d | J. Proteome Res. XXXX, XXX, XXX−XXX

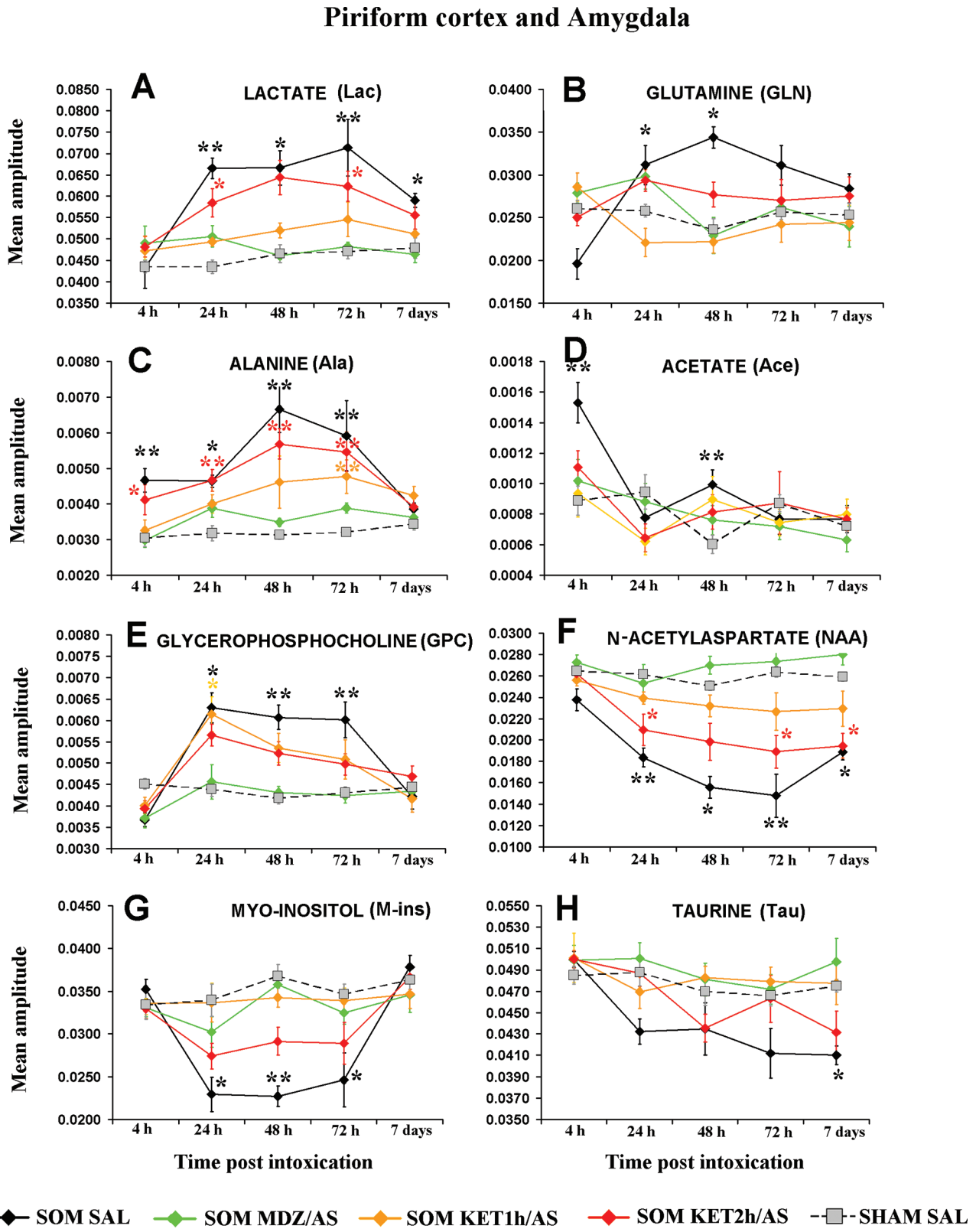

Figure 3. Evolution of mean metabolite amplitudes ± SEM from 4 h to 7 days after soman intoxication in PIR and AMG for the four SOM groups (solid line and full diamond) and the SHAM SAL group (dashed line and gray open square). Black, saline treatment (SAL); green, MDZ/AS treatment; orange, KET1h/AS treatment; red, KET2h/AS treatment. Groups were statistically compared by an ANOVA per ranks followed by a posthoc test: black ** $p < 0.01$, *$p < 0.05$ between SOM SAL and SHAM SAL groups; green ** $p < 0.01$, *$p < 0.05$ between SOM MDZ/AS and SHAM SAL; orange ** $p < 0.01$, *$p < 0.05$ between SOM KET1h/AS and SHAM SAL groups; and red ** $p < 0.01$, *$p < 0.05$ between SOM KET2h/AS and SHAM SAL groups. For the sake of clarity, all the statistical differences with SOM SAL group are omitted.

dx.doi.org/10.1021/pr300291d | J. Proteome Res. XXXX, XXX, XXX−XXX

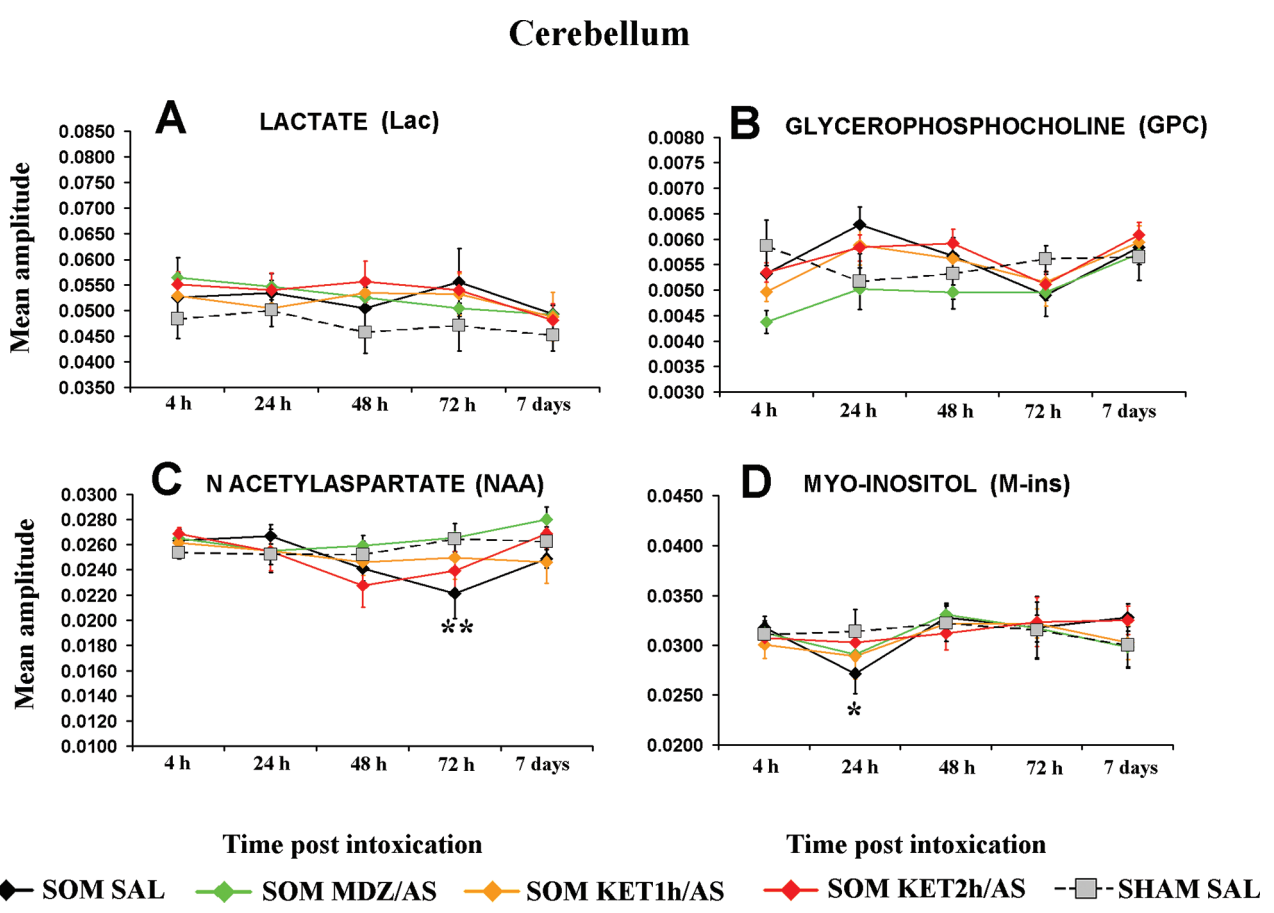

Figure 4. Evolution of mean metabolite amplitudes ± SEM from 4 h to 7 days after soman intoxication in CER for the four SOM groups (solid line and full diamond) and the SHAM SAL group (dashed line and gray open square). Black, saline treatment (SAL); green, MDZ/AS treatment; orange, KET1h/AS treatment; red, KET2h/AS treatment. Groups were statistically compared by an ANOVA per ranks followed by a posthoc test: black ** $p < 0.01$, *$p < 0.05$ between SOM SAL and SHAM SAL groups.

two treatment paradigms, the soman-induced changes in metabolite levels in CER were no longer detected.

Multivariate Statistical Analysis

Statistical Model of the Soman-Induced Metabolic Changes in PIR/AMG ("Soman Model"). The PCA analysis (data not shown) allowed us to identify four groups among the 102 observations (n = 57 from the present study and n = 45 from the previous study[27]). These groups were considered as Y classes for the PLS-DA analysis. They are labeled as follows: SHAM SAL for the class containing all nonintoxicated animals, SOM SAL 4 h for the class of animals euthanized 4 h post soman, SOM SAL 24−72 h for the class containing animals euthanized 24, 48, and 72 h after soman and finally SOM SAL 7 d for the group containing animals euthanized at day 7 after soman.

The observation of the score plot of our PLS-DA model provided a global view of all metabolic events. First, it showed a clear separation between SHAM SAL and SOM SAL classes (Figure 5A). Second, a hypothetical evolution pathway over time was suggested starting from SHAM SAL class and ending to SOM SAL 7 d class. Finally, it can be observed that SOM SAL 24−72 h and SHAM SAL classes are opposed relative to the first component axis, and that SOM SAL 7 d class is close to the SHAM SAL class.

Validation of the Model. Our PLS-DA model was built with three components and was characterized by a good fit (R^2Y = 0.64) and predictability (Q^2 = 0.62). As shown by permutation tests, no permuted value outperformed the original values either for R^2Y or Q^2. The Q^2-intercept was clearly negative, evidencing the absence of any overfit of the model for SHAM SAL (Figure 6A), SOM SAL 4 h, and SOM SAL 24−72 h classes. For SOM SAL 7 d group, some R^2Y and Q^2 values of permuted models were equivalent or greater than the original one (not shown). However, the CV-ANOVA test indicated highly significant ($p < 10^{-6}$) differences between classes.

Eight metabolites (variables) had a VIP > 1 (NAA, Ace, M-Ins, GPC, Lac, Ala, Gln and Tau), indicating their most important contribution in discriminating metabolic profiles between the four classes (Figure 6B). Moreover, the importance of variables in each class could be deduced from the observation of the loading scatter plot (Figure 6C). Two groups of variables were opposed along the first component: GPC, Lac and Gln on the left, associated with SOM SAL 24−72 h class and M-ins, NAA on the right, associated with SHAM SAL class. This indicates that variables in the first group were at their highest level in the SOM SAL 24−72 h class and that variables in the second group were at their lowest level in this class. Figure 6C also shows that Ace was at its highest level in the SOM SAL 4 h class.

Prediction of Treatment Efficacy Using the "Soman Model". As the statistical model described above presented a relatively good predictive power (Q^2 = 0.6), it was used to predict the efficacy of treatments (drug combinations and

dx.doi.org/10.1021/pr300291d | J. Proteome Res. XXXX, XXX, XXX−XXX

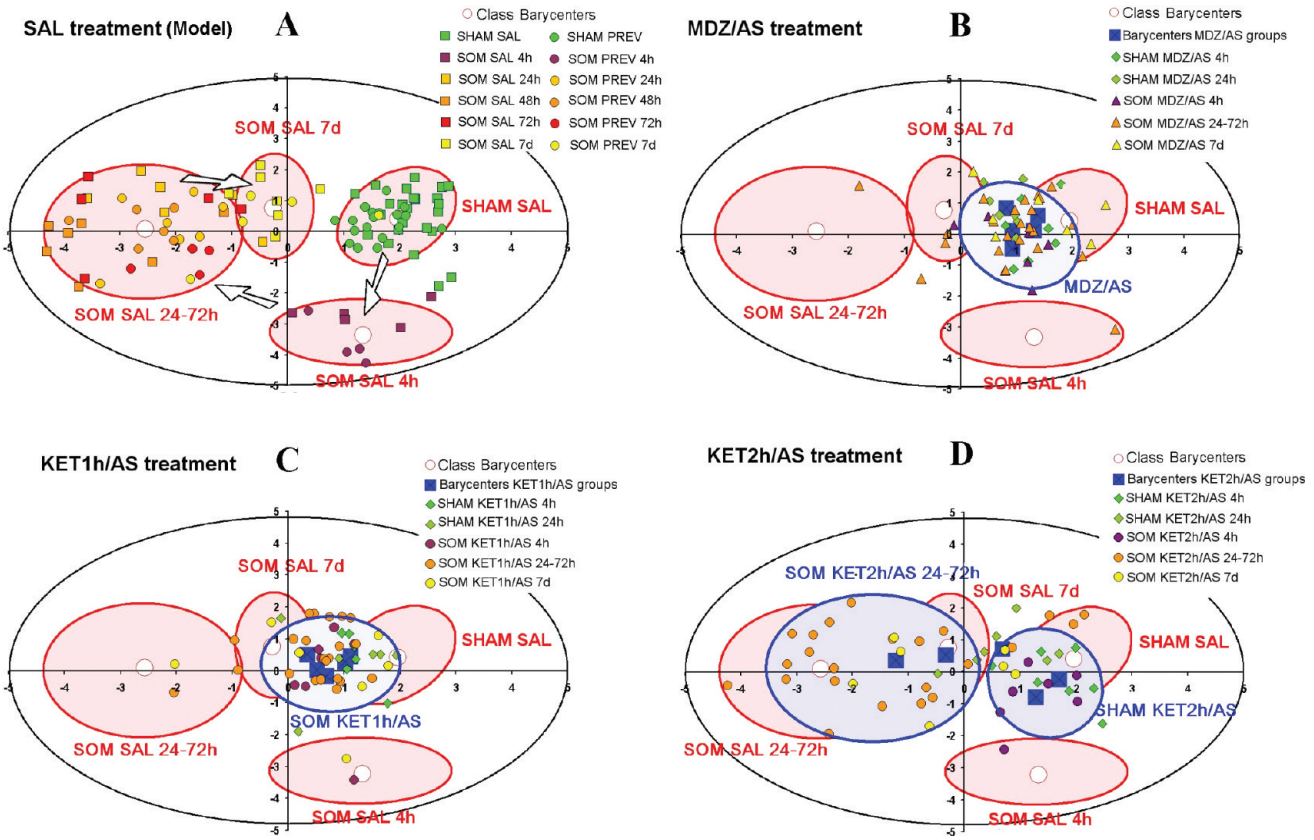

Figure 5. (A) "Soman model": First two components score plot of the PLS-DA model obtained using the quantitated metabolite amplitudes from PIR/AMG of SHAM SAL group (n = 25), SHAM from the previous (PREV) experiment (n = 18), SOM SAL group (n = 32), and SOM from previous experiment (n = 27). The red ellipses were drawn around observations of the four classes: "SHAM SAL" (green), "SOM SAL 4 h" (purple), "SOM SAL 24−72 h" (red and orange), and "SOM SAL 7 d" (yellow). The separation between classes is clearly observed. A hypothetical evolution pathway over time is suggested by the arrows. (B, C, D) Projection of treated animals, whether intoxicated or not (blue ellipses); the red ellipses represent the four classes of the "soman model" described in A.

timing of administration), considering that animals treated with the most efficient paradigm should be classified in the SHAM SAL group.

Score plot projections (Figure 5) and the classification table (Table 1) well synthesized the individual metabolic profiles and their normalization by treatments.

As expected, all animals of the SHAM MDZ/AS (Figure 5B), SHAM KET1h/AS (Figure 5C), SHAM KET2h/AS (Figure 5D) groups appeared in the immediate vicinity of the SHAM SAL class and had a high classification rate of 91−92% (Table 1). This well depicts the limited impact of the considered treatment paradigms on brain metabolism in nonintoxicated mice.

Concerning SOM groups, both the SOM MDZ/AS and SOM KET1h/AS mice were also projected close to the SHAM SAL class (Figure 5B,C), with more than respectively 84 and 76% of animals that could fit in this class (Table 1). In contrast, SOM KET2h/AS animals clearly differed from those of SHAM SAL (Figure 5D), and less than 35% of them were classified in the SHAM SAL class, while more than 50% had a metabolic profile of the SOM/SAL 24−72 h class (Table 1). This indicates that the delayed administration of KET/AS, 2 h postchallenge, appeared poorly effective to counteract soman-induced metabolism disturbances in the brain.

We can note that 4 h after intoxication, in the PLS-DA "soman model", very few animals (2/21) from MDZ/AS, KET1h/AS or KET2h/AS groups were found in the SOM SAL 4 h zone. At this time, all these animals were sedated or just out of anesthesia. This tends to confirm that the SOM SAL 4 h zone can be considered as a "seizure zone", a metabolic state specific to animals with long lasting seizures.

In the CER, no group appeared in the PCA analysis of metabolite concentrations. If the classes identified with PIR/AMG were used for the PLS-DA analysis of CER, no validated model could be found.

DISCUSSION

Using several approaches (clinical symptoms, quantitative brain histology and HRMAS NMR metabolic analysis), the present study was undertaken to increase the confidence in our previously published model[27] and to evaluate the impact of three treatment paradigms on the soman-induced brain metabolic changes: one immediate therapy known to be efficient (MDZ/AS) and two delayed therapies based on the combination of KET and AS. We tried to correlate the metabolic changes measured by proton HRMAS NMR to histopathological and clinical events.

Effect of Soman in the Absence of Any Treatment

Clinical Symptoms. All mice of the SOM SAL group (when they survived) showed, among other severe symptoms, long-lasting convulsions and drastic and durable loss of their body weight.

dx.doi.org/10.1021/pr300291d | J. Proteome Res. XXXX, XXX, XXX−XXX

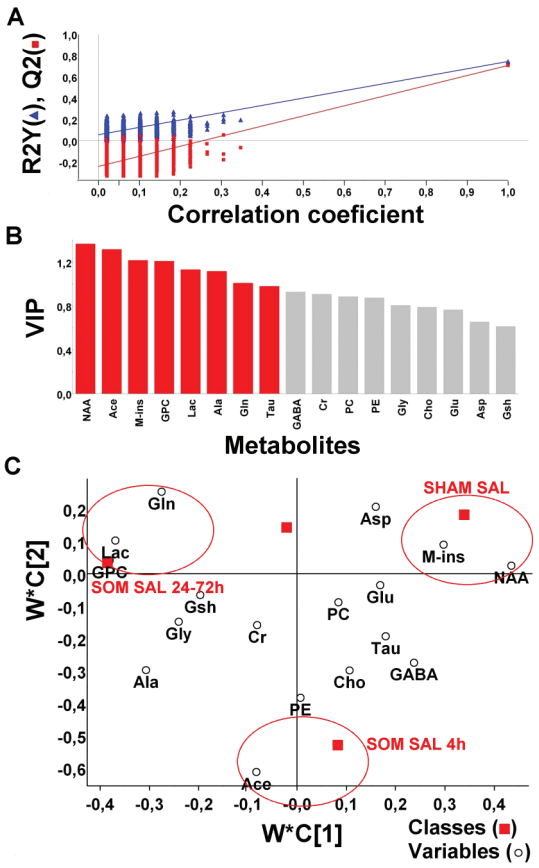

Figure 6. (A) Validation of the model for SHAM SAL class, using 999 permutations across three components. The regression line represents the correlation coefficient between the original and permutated *Y*-variables against R^2Y (green) and Q^2 (blue). (B) VIP plot: In red are represented the metabolites with a VIP > 1. (C) Loading plot of the model, showing variables and classes. Red ellipses regroup the most determinant metabolites (variables) associated with each class.

Table 1. Classification of Animals of the Treated Groups Using the PLS-DA "Soman Model"[a]

	classes of the "soman model"			
groups of treatment	SHAM SAL	SOM SAL 4 h	SOM SAL 24–72 h	SOM SAL 7 d
SHAM MDZ/AS	32/35 (91.4%)		1/35	2/35
SHAM KET1h/AS	32/35 (91.4%)	2/35		1/35
SHAM KET2h/AS	34/37 (91.9%)		3/37	1/37
SOM MDZ/AS	31/37 (83.8%	2/37	3/37	1/37
SOM KET1h/AS	28/37 (75.7%)	2/37	5/37	2/37
SOM KET2h/AS	14/41 (34.1%)	1/41	22/41	4/41

[a]The rate of classification in the SHAM SAL group (in brackets) is considered as a criterion for the evaluation of treatment efficacy.

Despite the lack of EEG recording in the present study, our clinical evaluation of the absence/presence/disappearance of convulsions can be trustfully interpreted in terms of absence/presence/disappearance of actual electrographic seizure activity. This assertion is based on (i) the available bibliographic data (references in the Introduction section and in the following paragraphs) and (ii) our measurement of the body weight loss that is a recognized indicator of soman-induced brain damage[9,41,53,59] and thus of long-lasting seizure activity owing to the relationship between the two events.[5,53,60,61] Although during MDZ or KET sedation, the absence of convulsions cannot be only interpreted as the termination of seizures, the prevention of brain damage is a good indicator of their action on seizures.

Histology and Metabolism. PIR and AMG, two brain areas known to be extremely sensitive to soman brain damaging effects,[4−7] expectedly showed profound structural changes as evidenced by the presence of numerous eosinophilic cells.

In the AMG, the number of damaged cells, as evidenced by HP staining, peaked during the first three days before declining. Such observation is also similar to the results obtained by others in soman-intoxicated rats and mice;[7] this decrease of damaged cells, after the third day, is mostly caused by the disappearance of the damaged cells rather than by their recovery,[7] although this can only be ascertained by a precise cell counting. In the same brain area, no astrocyte activation was discernible at 24 h. In literature, the delay for the induction of GFAP after soman poisoning is not clearly established. Indeed, some works indicated a rapid activation of astroglia within the very first hours following challenge, as evidenced by the increase in GFAP mRNA[62,63] or even GFAP immunoreactivity.[14] In this last work, however, the animals had been operated a week before soman poisoning, and this may well have induced an astroglial activation. On the other hand, our results are well coherent with those of others evidencing a weak or absent GFAP immunoreactivity in the AMG or PIR before 2−3 days, and an important increase of GFAP immunoreactivity at day 7 after soman exposure.[4,13]

In the PIR, the number of eosinophilic cells at 24−72 h was less important than in the AMG at the same time points but, instead of further decreasing, continued to increase until day 7. As revealed by GFAP immunohistochemistry, astrocyte activation was weak the third day of the intoxication and strongly increased at day 7. All these results suggest that structural damage and accompanying astrogliosis in the PIR were apparently delayed compared to the AMG. To our knowledge, such a phenomenon has never been reported so far.

Soman-induced changes on PIR and AMG metabolism were not distinguished in this study, but globally, a parallelism with the histological data was observed. The Lac level seemed to well fit with the number of acidophilic cells (HP staining) in AMG, with a large increase from 24 to 72 h and a partial recovery at day 7. It is tempting to link these two perturbations since lactate has been reported to be involved in tissular acidosis.[64] However, this was not fully confirmed in PIR, where acidophilic staining was increased at day 7 but not followed by an increase of the Lac level.

The NAA decrease closely followed the inverse kinetics of Lac. A decrease of this metabolite has already been reported to be associated with a deficit in mitochondrial activity[32] but it may also be related to neuronal death.[65] Extending the duration of the study beyond 7 days might help to know the relative contribution of these two events.

At day 7, the astrocyte activation was high in AMG and PIR, while most of the metabolites recovered their control level except Lac, NAA and Tau. The Tau level slowly decreased after

dx.doi.org/10.1021/pr300291d | J. Proteome Res. XXXX, XXX, XXX−XXX

24 h post soman, and this decrease became significant at day 7. In a mouse model of kainate-induced SE, an increase of Tau rather than a decrease was observed in the hippocampus at day 7.[66] More in the line of our data are the reports of antiepileptic effects of taurine treatments owing to the effects of Tau on neuronal excitability and on the modulation of recurrent seizure activity.[67,68] Tau was also studied in a model of long-term effects of kainate-induced seizures in rats (6 months) of less relevance to our study.[35] However a decrease in AMG/PIR was also reported. Therefore, a more focused study would be necessary to test if the decrease in Tau levels we observed may have functional consequences and facilitate recurrent seizures.

At difference to AMG/PIR, the CER appeared free of any detectable damage (HP staining) and astrocytic activation. This observation is well in line with that of others showing that, at least in soman poisoned rodents, damage to this structure are either rare and limited to the vermis[5,6] or even absent.[7] CER also presented very little changes in metabolism confirming our previous results.[27] Only NAA significantly decreased 72 h after intoxication with a recovery at day 7. To the best of our knowledge, data on OP-induced changes in CER are limited. We reported some inflammatory gene response changes in a comparable mouse model.[16] Some more delayed modifications of cellular signaling have also been reported.[69] All in all, this clearly shows that CER cannot be considered as devoid of any changes.

PLS-DA "Soman Model". The PLS-DA model of soman-induced metabolic changes, built with HRMAS NMR metabolic data, provides a synthetic view of all the metabolic events occurring during the soman intoxication. It is in accordance with our previous work,[27] even if slight differences are observed in this study for some metabolites. The score plot and the loading plot show that there is a good agreement between the classification of metabolic profiles and the clinical observations, body weight or histopathology. More specifically, the first component of the model clearly separates SHAM SAL and SOM SAL 24−72 h classes. The latter corresponds to the period when brain lesions, cerebral edema and neuro-inflammation become more pronounced. It appears like a "neuropathological zone", with high levels of GPC, Lac and Gln, and low levels of NAA and M-ins. The second component mainly separates SOM SAL 4 h class from the others. This class is characterized by a high level of Ace, a metabolite that is not abundant in normal brain. Since animals have fully developed epileptic activity at that time point, this graphic zone could be considered as the "seizure zone". The third component allows separating SOM SAL 7 d from the other classes. A normalization of most of the metabolites is observed at this time point, and the difference with SHAM SAL mice is mainly due to NAA and Tau levels, which remain slightly decreased. This class regroups mice that are recovering.

In a second step, we thus challenged our model with the results obtained after treatment with anticonvulsant combinations.

Effect of Treatments on Soman-Intoxicated Mice

MDZ/AS Treatment. An immediate treatment with a MDZ/AS combination prevented the appearance of convulsions and clearly the loss in body weight of the animals. This was paralleled by a good histological neuroprotection (neither detectable brain damage nor astrocyte activation) as well as by a good protection against the soman-induced metabolic changes, both in CER and in PIR/AMG. Furthermore, using the PLS-DA "soman model", it appeared as the most efficient treatment, with 84% of observations classified in the SHAM SAL group. From a methodological point of view, these mice constituted a very good positive control for the evaluation of the efficacy of the other treatments. This confirms that MDZ/AS, when administered within minutes after soman intoxication, is an efficient antidote against the central effects of the poisoning and is capable to prevent seizures and related brain damage.[40,53,70,71]

KET1h/AS Treatment. During SE, benzodiazepines are usually ineffective, and combinations of KET have proven their efficacy in different animal models such as guinea pigs[51] as well as mice.[15] Administration of KET/AS 1 h postchallenge produced almost an immediate arrest of ongoing convulsions. Without EEG recording, it is not possible to ascertain that the seizures were also abated but the loss of body weight being limited, this is highly probable. Although the recovery in body weight at day 7 was less pronounced than after an immediate treatment with MDZ/AS, the body weight was not significantly different from that of the SHAM groups. Administration of KET/AS in poisoned animals also did not prove more deleterious than in nonpoisoned animals (death rate 7 and 8% respectively), showing that at an appropriate dosage, KET can be used in poisoned individuals. Like in Dhote et al.,[15] the paradigms were here chosen to be proofs of concept. In histological sections, the number of eosinophilic cells in sensitive brain areas (AMG, PIR) was considerably reduced compared to that in the SOM SAL group. Moreover, the treatment strongly reduced most of the soman-induced metabolic changes in PIR/AMG or CER. Using the PLS-DA "soman model" (for PIR/AMG), 76% of the observations were classified in the SHAM SAL group. All these observations are thus consistent with our previous data on KET/AS combinations.[15,51,52] In these previous papers, we also mentioned that the neuroprotection was not complete. Here also, some perturbations could still be observed in PIR/AMG of the treated animals, e.g., in the levels of Ala, NAA and GPC, or in astrogliosis. Indeed, an important astrocytic activation was still evidenced at 72 h with a magnitude comparable to that detected at the same time in the SOM SAL group. Conversely, at day 7, KET/AS treatment could almost totally reduce GFAP immunoreactivity to the level of controls. Very comparable results were obtained at 48 h and 7 days with slightly different KET/AS paradigms in a comparable mouse model.[15] That seems to indicate that KET/AS, maybe because of the delay in administration, could not prevent the initiation of astrogliosis but markedly reduced its duration. Interestingly, a similar effect of KET/AS was observed on the GPC levels: while KET/AS could not prevent its increase at 24 h, the treatment apparently contributed to a faster return to control level.

Astrogliosis may be initiated by pro-inflammatory cytokines even in the absence of cellular damage.[72−74] We previously hypothesized that the GPC increase may also be related to the activation of different pro-inflammatory enzymes.[27] KET/AS clearly counteracted soman-induced neuroinflammation 48 h and 7 days postchallenge,[15] but data are lacking regarding the possible effects of these combinations on the early pro-inflammatory signals.

Globally, a delayed administration of KET/AS could, for many of the parameters, be as effective as an immediate treatment with MDZ/AZ. However, 1 h of fully developed seizures before KET/AS administration had an obvious impact, and in the PLS-DA "soman model", the KET1h/AS mice were

dx.doi.org/10.1021/pr300291d | J. Proteome Res. XXXX, XXX, XXX−XXX

projected near the SHAM SAL zone but were more scattered than the MDZ/AS mice, and a few points even appeared in the SOM SAL 24−72 h class.

KET2h/AS Treatment. By further delaying the initiation of treatment with KET/AS to 2 h postchallenge, a reduced neuroprotection was anticipated as described earlier.[51,52] This was fully confirmed in the present study. The delayed administration of KET/AS only transiently stopped the convulsions in spite of repeated injections. These long-lasting seizures had a clear impact on the body weight loss that was comparable to that of untreated mice. The neuroprotection was indeed partial, with numerous eosinophilic cells and an extended astrogliosis still present although less prominent than that observed in untreated poisoned animals. The metabolic perturbations induced by the administration of soman were observed, but they were slightly reduced by the treatment. As a consequence, in the score plot of the PLS-DA "soman model", the KET2h/AS treated mice were largely scattered, with many observations in the SOM SAL 24−72 h zone, reflecting the low efficacy of the treatment on the changes in brain metabolism.

CONCLUSION

Using proton HRMAS NMR of mouse brain biopsies, we have established a statistical model that synthesizes all the metabolic events occurring in some areas of the brain during 7 days after soman intoxication. In this model, "control" and "pathological zones" are clearly separated. Moreover, classification with this model is robust, and the efficiency of neuroprotective treatments can be globally evaluated by the classification of treated animals in the different zones. Our results show that animals that follow the entire "soman model" pathway or that enter in the "pathological zone" will suffer from brain consequences of soman intoxication.

Analysis of the individual variations of each metabolite, associated with a histological approach, could help to better understand the complex pathophysiological events occurring during the intoxication and may provide leads to elaborate further treatments. Further experiments should also focus on the changes in metabolism occurring beyond 7 days, e.g., in order to confirm or not the recovery of NAA, Lac or Tau. The hypothetical link between GPC and inflammation has to be more precisely investigated. Metabolic profiling using HRMAS NMR data thus provides an interesting diagnostic and predictive tool for the experimental evaluation of the cerebral consequences of nerve agent poisoning and treatments. Moreover, these findings could be very useful to improve the potential of in vivo proton magnetic resonance spectroscopy as a noninvasive diagnostic tool in humans.

Finally, the present work also supports further the anticonvulsant and neuroprotective efficacy of a KET/AS combination during refractory SE, its effect being comparable but not entirely similar to that of an immediate treatment with a benzodiazepine. Approximately 1 h of soman-induced seizures still remains the limit of this treatment as demonstrated by the poor neuroprotection afforded by KET/AS given 2 h postchallenge. Extending further the delay before a given treatment is especially important since such delays may be expected because of confusion in battle or in the aftermath of a terrorist attack, the two main circumstances where nerve agents such as soman might be used.

AUTHOR INFORMATION

Corresponding Author

*Tel.: (33) 4 76 63 69 67. Fax: (33) 4 76 63 69 22. E-mail: Florence.fauvelle@free.fr.

Notes

The authors declare no competing financial interest.

ACKNOWLEDGMENTS

This work was supported by a grant from the Direction Générale de l'Armement (DGA; Contract No. 08co502 to F.D.).

REFERENCES

(1) McDonough, J. H., Jr.; Shih, T. M. Neuropharmacological mechanisms of nerve agent-induced seizure and neuropathology. *Neurosci. Biobehav. Rev.* **1997**, *21* (5), 559−79.

(2) Lallement, G.; Carpentier, P.; Collet, A.; Baubichon, D.; Pernot Marino, I.; Blanchet, G. Extracellular acetylcholine changes in rat limbic structures during soman- induced seizures. *Neurotoxicology* **1992**, *13* (3), 557−68.

(3) Sloviter, R. S.; Dempster, D. W. "Epileptic" brain damage is replicated qualitatively in the rat hippocampus by central injection of glutamate or aspartate but not by GABA or acetylcholine. *Brain Res. Bull.* **1985**, *15* (1), 39−60.

(4) Baille, V.; Clarke, P. G.; Brochier, G.; Dorandeu, F.; Verna, J. M.; Four, E.; Lallement, G.; Carpentier, P. Soman-induced convulsions: the neuropathology revisited. *Toxicology* **2005**, *215* (1−2), 1−24.

(5) Carpentier, P.; Delamanche, I. S.; Le Bert, M.; Blanchet, G.; Bouchaud, C. Seizure-related opening of the blood-brain barrier induced by soman: possible correlation with the acute neuropathology observed in poisoned rats. *Neurotoxicology* **1990**, *11* (3), 493−508.

(6) Lemercier, G.; Carpentier, P.; Sentenac-Roumanou, H.; Morelis, P. Histological and histochemical changes in the central nervous system of the rat poisoned by an irreversible anticholinesterase organophosphorus compound. *Acta Neuropathol.* **1983**, *61* (2), 123−9.

(7) McDonough, J. H., Jr.; Clark, T. R.; Slone, T. W., Jr.; Zoeffel, D.; Brown, K.; Kim, S.; Smith, C. D. Neural lesions in the rat and their relationship to EEG delta activity following seizures induced by the nerve agent soman. *Neurotoxicology* **1998**, *19* (3), 381−92.

(8) de Araujo Furtado, M.; Lumley, L. A.; Robison, C.; Tong, L. C.; Lichtenstein, S.; Yourick, D. L. Spontaneous recurrent seizures after status epilepticus induced by soman in Sprague−Dawley rats. *Epilepsia* **2010**, *7*, 7.

(9) Filliat, P.; Coubard, S.; Pierard, C.; Liscia, P.; Beracochea, D.; Four, E.; Baubichon, D.; Masqueliez, C.; Lallement, G.; Collombet, J. M. Long-term behavioral consequences of soman poisoning in mice. *Neurotoxicology* **2007**, *28* (3), 508−19.

(10) McDonough, J. H., Jr.; Smith, R. F.; Smith, C. D. Behavioral correlates of soman-induced neuropathology: deficits in DRL acquisition. *Neurobehav. Toxicol. Teratol.* **1986**, *8* (2), 179−87.

(11) Testylier, G.; Lahrech, H.; Montigon, O.; Foquin, A.; Delacour, C.; Bernabe, D.; Segebarth, C.; Dorandeu, F.; Carpentier, P. Cerebral edema induced in mice by a convulsive dose of soman. Evaluation through diffusion-weighted magnetic resonance imaging and histology. *Toxicol. Appl. Pharmacol.* **2007**, *220*, 125−37.

(12) Carpentier, P.; Testylier, G.; Baille, V.; Foquin, A.; Delacour, C.; Dorandeu, F. Cerebral edema in soman poisoning. In *The Neurochemical Consequences of Organophosphate Poisoning in the CNS*; Raveh, B. A. W. L., Ed.; Transworld Research Network: Kerala, India, 2010; pp 1−17.

(13) Collombet, J. M.; Four, E.; Bernabe, D.; Masqueliez, C.; Burckhart, M. F.; Baille, V.; Baubichon, D.; Lallement, G. Soman poisoning increases neural progenitor proliferation and induces long-term glial activation in mouse brain. *Toxicology* **2005**, *208* (3), 319−34.

(14) Zimmer, L. A.; Ennis, M.; Shipley, M. T. Soman-induced seizures rapidly activate astrocytes and microglia in discrete brain regions. *J. Comp. Neurol.* **1997**, *378* (4), 482−92.
(15) Dhote, F.; Carpentier, P.; Barbier, L.; Peinnequin, A.; Baille, V.; Pernot, F.; Testylier, G.; Beaup, C.; Foquin, A.; Dorandeu, F. Combinations of ketamine and atropine are neuroprotective and reduce neuroinflammation after a toxic status epilepticus in mice. *Toxicol. Appl. Pharmacol.* **2012**, *256*, 195−209.
(16) Dhote, F.; Peinnequin, A.; Carpentier, P.; Baille, V.; Delacour, C.; Foquin, A.; Lallement, G.; Dorandeu, F. Prolonged inflammatory gene response following soman-induced seizures in mice. *Toxicology* **2007**, *238* (2−3), 166−76.
(17) Svensson, I.; Waara, L.; Johansson, L.; Bucht, A.; Cassel, G. Soman-induced interleukin-1 beta mRNA and protein in rat brain. *Neurotoxicology* **2001**, *22* (3), 355−62.
(18) Williams, A. J.; Berti, R.; Yao, C.; Price, R. A.; Velarde, L. C.; Koplovitz, I.; Schultz, S. M.; Tortella, F. C.; Dave, J. R. Central neuroinflammatory gene response following soman exposure in the rat. *Neurosci. Lett.* **2003**, *349* (3), 147−50.
(19) Ebisu, T.; Rooney, W. D.; Graham, S. H.; Mancuso, A.; Weiner, M. W.; Maudsley, A. A. MR spectroscopic imaging and diffusion-weighted MRI for early detection of kainate-induced status epilepticus in the rat. *Magn. Reson. Med.* **1996**, *36* (6), 821−8.
(20) Najm, I. M.; Wang, Y.; Shedid, D.; Luders, H. O.; Ng, T. C.; Comair, Y. G. MRS metabolic markers of seizures and seizure-induced neuronal damage. *Epilepsia* **1998**, *39* (3), 244−50.
(21) van Gelder, N. M.; Sherwin, A. L. Metabolic parameters of epilepsy: adjuncts to established antiepileptic drug therapy. *Neurochem. Int.* **2003**, *28* (2), 353−65.
(22) Pazdernik, T. L.; Cross, R.; Giesler, M.; Nelson, S.; Samson, F.; McDonough, J., Jr. Delayed effects of soman: brain glucose use and pathology. *Neurotoxicology* **1985**, *6* (3), 61−70.
(23) Nguyen, N.; Gonzalez, S. V.; Rise, F.; Hassel, B. Cerebral metabolism of glucose and pyruvate in soman poisoning. A (13)C nuclear magnetic resonance spectroscopic study. *Neurotoxicology* **2007**, *28* (1), 13−8.
(24) Fosbraey, P.; Wetherell, J. R.; French, M. C. Neurotransmitter changes in guinea-pig brain regions following soman intoxication. *J. Neurochem.* **1990**, *54* (1), 72−79.
(25) Bodjarian, N.; Carpentier, P.; Blanchet, G.; Baubichon, D.; Lallement, G. Cholinergic activation of phosphoinositide metabolism during soman-induced seizures. *Neuroreport* **1993**, *4* (10), 1191−3.
(26) Filbert, M. G.; Forster, J. S.; Phann, S.; Ballough, G. P. Effects of soman-induced convulsions on phosphoinositide metabolism. *Mol. Chem. Neuropathol.* **1998**, *33* (1), 1−14.
(27) Fauvelle, F.; Dorandeu, F.; Carpentier, P.; Foquin, A.; Rabeson, H.; Graveron-Demilly, D.; Arvers, P.; Testylier, G. Changes in mouse brain metabolism following a convulsive dose of soman: A proton HRMAS NMR study. *Toxicology* **2010**, *267*, 99−111.
(28) Ben Sellem, D.; Elbayed, K.; Neuville, A.; Moussallieh, F. M.; Lang-Averous, G.; Piotto, M.; Bellocq, J. P.; Namer, I. J. Metabolomic characterization of ovarian epithelial carcinomas by HRMAS-NMR spectroscopy. *J. Oncol.* **2011**, *2011*, 174019.
(29) Borel, M.; Pastoureau, P.; Papon, J.; Madelmont, J. C.; Moins, N.; Maublant, J.; Miot-Noirault, E. Longitudinal profiling of articular cartilage degradation in osteoarthritis by high-resolution magic angle spinning ^{1}H NMR spectroscopy: experimental study in the meniscectomized guinea pig model. *J. Proteome Res.* **2009**, *8* (5), 2594−600.
(30) Martin, F. P.; Wang, Y.; Sprenger, N.; Holmes, E.; Lindon, J. C.; Kochhar, S.; Nicholson, J. K. Effects of probiotic *Lactobacillus paracasei* treatment on the host gut tissue metabolic profiles probed via magic-angle-spinning NMR spectroscopy. *J. Proteome Res.* **2007**, *6* (4), 1471−81.
(31) Pfisterer, W. K.; Nieman, R. A.; Scheck, A. C.; Coons, S. W.; Spetzler, R. F.; Preul, M. C. Using ex vivo proton magnetic resonance spectroscopy to reveal associations between biochemical and biological features of meningiomas. *Neurosurg. Focus* **2010**, *28* (1), E12.
(32) Moffett, J. R.; Ross, B.; Arun, P.; Madhavarao, C. N.; Namboodiri, A. M. *N*-Acetylaspartate in the CNS: from neurodiagnostics to neurobiology. *Prog. Neurobiol.* **2007**, *81* (2), 89−131.
(33) Gupta, R. C.; Milatovic, D.; Dettbarn, W. D. Depletion of energy metabolites following acetylcholinesterase inhibitor-induced status epilepticus: Protection by antioxidants. *NeuroToxicology* **2001**, *22* (2), 271−82.
(34) Sterns, R. H.; Silver, S. M. Brain volume regulation in response to hypo-osmolality and its correction. *Am. J. Med.* **2006**, *119* (7 Suppl 1), S12−6.
(35) Baran, H. Alterations of taurine in the brain of chronic kainic acid epilepsy model. *Amino Acids* **2006**, *31* (3), 303−7.
(36) Chapman, S.; Kadar, T.; Gilat, E. Seizure duration following sarin exposure affects neuro-inflammatory markers in the rat brain. *Neurotoxicology* **2006**, *27* (2), 277−83.
(37) Martin, L. J.; Doebler, J. A.; Shih, T. M.; Anthony, A. Protective effect of diazepam pretreatment on soman-induced brain lesion formation. *Brain Res.* **1985**, *325* (1−2), 287−9.
(38) Lipp, J. A. Effect of benzodiazepine derivatives on soman-induced seizure activity and convulsions in the monkey. *Arch. Int. Pharmacodyn. Ther.* **1973**, *202* (2), 244−51.
(39) Clement, J. G.; Broxup, B. Efficacy of diazepam and avizafone against soman-induced neuropathology in brain of rats. *Neurotoxicology* **1993**, *14* (4), 485−504.
(40) McDonough, J. H., Jr.; McMonagle, J.; Copeland, T.; Zoeffel, D.; Shih, T. M. Comparative evaluation of benzodiazepines for control of soman-induced seizures. *Arch. Toxicol.* **1999**, *73* (8−9), 473−8.
(41) Myhrer, T.; Andersen, J. M.; Nguyen, N. H.; Aas, P. Soman-induced convulsions in rats terminated with pharmacological agents after 45 min: Neuropathology and cognitive performance. *Neurotoxicology* **2005**, *26* (1), 39−48.
(42) Shih, T. M. Anticonvulsant effects of diazepam and MK-801 in soman poisoning. *Epilepsy Res.* **1990**, *7* (2), 105−16.
(43) Sparenborg, S.; Brennecke, L. H.; Jaax, N. K.; Braitman, D. J. Dizocilpine (MK-801) arrests status epilepticus and prevents brain damage induced by soman. *Neuropharmacology* **1992**, *31* (4), 357−68.
(44) Carpentier, P.; Foquin, A.; Kamenka, J. M.; Rondouin, G.; Lerner Natoli, M.; de Groot, D. M.; Lallement, G. Effects of thienylphencyclidine (TCP) on seizure activity and brain damage produced by soman in guinea-pigs: ECoG correlates of neurotoxicity. *Neurotoxicology* **2001**, *22* (1), 13−28.
(45) Carpentier, P.; Foquin Tarricone, A.; Bodjarian, N.; Rondouin, G.; Lerner Natoli, M.; Kamenka, J. M.; Blanchet, G.; Denoyer, M.; Lallement, G. Anticonvulsant and antilethal effects of the phencyclidine derivative TCP in soman poisoning. *Neurotoxicology* **1994**, *15* (4), 837−52.
(46) Lallement, G.; Baubichon, D.; Clarencon, D.; Galonnier, M.; Peoch, M.; Carpentier, P. Review of the value of gacyclidine (GK-11) as adjuvant medication to conventional treatments of organophosphate poisoning: Primate experiments mimicking various scenarios of military or terrorist attack by soman. *Neurotoxicology* **1999**, *20* (4), 675−84.
(47) Abend, N. S.; Dlugos, D. J. Treatment of refractory status epilepticus: literature review and a proposed protocol. *Pediatr. Neurol.* **2008**, *38* (6), 377−90.
(48) Dorandeu, F.; Carpentier, P.; Baille, V.; Dhote, F.; Testylier, G.; Pernot, F.; Mion, G.; Rüttimann, M.; Lallement, G. Field treatment of soman-induced self-sustaining status epilepticus. Are ketamine and other NMDA antagonists the only options? In *The Neurochemical Consequences of Organophosphate Poisoning in the CNS*; Raveh, B. A. W. L., Ed.; Transworld Research Network: Kerala, India, 2010; pp 149−83.
(49) Sun, J.; Wang, X. D.; Liu, H.; Xu, J. G. Ketamine suppresses endotoxin-induced NF-kappaB activation and cytokines production in the intestine. *Acta Anaesthesiol. Scand.* **2004**, *48* (3), 317−21.
(50) Taniguchi, T.; Yamamoto, K. Anti-inflammatory effects of intravenous anesthetics on endotoxemia. *Mini-Rev. Med. Chem.* **2005**, *5* (3), 241−5.

(51) Dorandeu, F.; Carpentier, P.; Baubichon, D.; Four, E.; Bernabe, D.; Burckhart, M. F.; Lallement, G. Efficacy of the ketamine-atropine combination in the delayed treatment of soman-induced status epilepticus. *Brain Res.* **2005**, *1051* (1−2), 164−75.
(52) Dorandeu, F.; Baille, V.; Mikler, J.; Testylier, G.; Lallement, G.; Sawyer, T. W.; Carpentier, P. Protective effects of S(+) ketamine and atropine against lethality and brain damage during soman-induced status epilepticus in guinea-pigs. *Toxicology* **2007**, *234* (3), 185−93.
(53) McDonough, J. H., Jr.; Jaax, N. K.; Crowley, R. A.; Mays, M. Z.; Modrow, H. E. Atropine and/or diazepam therapy protects against soman-induced neural and cardiac pathology. *Fundam. Appl. Toxicol.* **1989**, *13* (2), 256−276.
(54) Paxinos, G.; Franklin, K. *The Mouse Brain in Stereotaxic Coordinates*; Academic Press Inc: New York, 1997.
(55) Rabeson, H.; Fauvelle, F.; Testylier, G.; Foquin, A.; Carpentier, P.; Dorandeu, F.; Ormondt, D. v.; Graveron-Demilly, D. Quantitation with QUEST of brain HRMAS-NMR signals: application to metabolic disorders in experimental epileptic seizures. *Magn. Reson. Med.* **2008**, *59* (6), 1266−73.
(56) Ratiney, H.; Sdika, M.; Coenradie, Y.; Cavassila, S.; van, O. D.; Graveron-Demilly, D. Time-domain semi-parametric estimation based on a metabolite basis set. *NMR Biomed.* **2005**, *18* (1), 1−13.
(57) Tenenhaus, M. *Régression PLS: Théorie et Pratique*; Technip: Paris, 1998.
(58) Westerhuis, J. A.; Hoefsloot, H. C.; Smit, S.; Vis, D. J.; Smilde, A. K.; van Velzen, E. J.; van Duijnhoven, J. P. M.; van Dorsten, F. A. Assessment of PLSDA cross validation. *Metabolomics* **2008**, *4*, 81−9.
(59) Churchill, L.; Pazdernik, T. L.; Jackson, J. L.; Nelson, S. R.; Samson, F. E.; McDonough, J., Jr.; McLeod, C., Jr. Soman-induced brain lesions demonstrated by muscarinic receptor autoradiography. *Neurotoxicology* **1985**, *6* (3), 81−90.
(60) Carpentier, P.; Foquin, A.; Dorandeu, F.; Lallement, G. Delta activity as an early indicator for soman-induced brain damage: A review. *Neurotoxicology* **2001**, *22* (3), 299−315.
(61) Carpentier, P.; Foquin, A.; Rondouin, G.; Lerner Natoli, M.; De Groot, D. M. G.; Lallement, G. Effects of atropine sulphate on seizure activity and brain damage produced by soman in guinea-pigs: ECoG correlates of neuropathology. *Neurotoxicology* **2000**, *21* (4), 521−40.
(62) Baille Le Crom, V.; Collombet, J. M.; Carpentier, P.; Brochier, G.; Burckhart, M. F.; Foquin, A.; Pernot Marino, I.; Rondouin, G.; Lallement, G. Early regional changes of GFAP mRNA in rat hippocampus and dentate gyrus during soman-induced seizures. *NeuroReport* **1995**, *7* (1), 365−9.
(63) Damodaran, T. V.; Bilska, M. A.; Rahman, A. A.; Abou-Doni, M. B. Sarin causes early differential alteration and persistent over-expression in mRNAs coding for glial fibrillary acidic protein (GFAP) and vimentin genes in the central nervous system of rats. *Neurochem. Res.* **2002**, *27* (5), 407−15.
(64) Sun, P. Z.; Cheung, J. S.; Wang, E.; Lo, E. H. Association between pH-weighted endogenous amide proton chemical exchange saturation transfer MRI and tissue lactic acidosis during acute ischemic stroke. *J. Cereb. Blood Flow Metab.* **2011**, *31* (8), 1743−50.
(65) Tokumitsu, T.; Mancuso, A.; Weinstein, P. R.; Weiner, M. W.; Naruse, S.; Maudsley, A. A. Metabolic and pathological effects of temporal lobe epilepsy in rat brain detected by proton spectroscopy and imaging. *Brain Res.* **1997**, *744* (1), 57−67.
(66) Junyent, F.; De Lemos, L.; Utrera, J.; Paco, S.; Aguado, F.; Camins, A.; Pallas, M.; Romero, R.; Auladell, C. Content and traffic of taurine in hippocampal reactive astrocytes. *Hippocampus* **2011**, *2*, 185−97.
(67) L'Amoreaux, W. J.; Marsillo, A.; El Idrissi, A. Pharmacological characterization of GABAA receptors in taurine-fed mice. *J. Biomed. Sci.* **2010**, *17* (Suppl 1), S14.
(68) Junyent, F.; Utrera, J.; Romero, R.; Pallas, M.; Camins, A.; Duque, D.; Auladell, C. Prevention of epilepsy by taurine treatments in mice experimental model. *J. Neurosci. Res.* **2009**, *87* (6), 1500−8.
(69) Pejchal, J.; Osterreicher, J.; Kassa, J.; Tichy, A.; Micuda, S.; Sinkorova, Z.; Zarybnicka, L. Soman poisoning alters p38 MAPK pathway in rat cerebellar Purkinje cells. *J. Appl. Toxicol.* **2009**, *29* (4), 338−45.
(70) Koplovitz, I.; Schulz, S.; Shutz, M.; Railer, R.; Macalalag, R.; Schons, M.; McDonough, J. Combination anticonvulsant treatment of soman-induced seizures. *J. Appl. Toxicol.* **2001**, *21* (Suppl 1), 53−5.
(71) Shih, T.-M.; Duniho, S. M.; McDonough, J. H. Control of nerve agent-induced seizures is critical for neuroprotection and survival. *Toxicol. Appl. Pharmacol.* **2003**, *188* (2), 69−80.
(72) Vezzani; Baram, T. Z. New roles for interleukin-1 beta in the mechanisms of epilepsy. *Epilepsy Curr.* **2007**, *7* (2), 45−50.
(73) Vezzani; Conti, M.; De Luigi, A.; Ravizza, T.; Moneta, D.; Marchesi, F.; De Simoni, M. G. Interleukin-1beta immunoreactivity and microglia are enhanced in the rat hippocampus by focal kainate application: functional evidence for enhancement of electrographic seizures. *J. Neurosci.* **1999**, *19* (12), 5054−65.
(74) Vezzani, A.; Granata, T. Brain inflammation in epilepsy: experimental and clinical evidence. *Epilepsia* **2005**, *46* (11), 1724−43.